web of semantic

Journal of Interdisciplinary Science

Research Article Peer-review, Open Access

Adaptive Handover Framework between NOMA and OFDM for Enhanced Bandwidth Efficiency in Fading Cellular Channels

Pratik Brahmbhatt [1]**,**

Abstract

With the proliferation of users and multimedia services, optimizing bandwidth efficiency has become pivotal in modern cellular networks. Bandwidth remains a finite and shared resource; therefore, innovative strategies are needed to maximize spectral utilization. This paper introduces an adaptive hybrid system that integrates Non-Orthogonal Multiple Access (NOMA) with Orthogonal Frequency Division Multiplexing (OFDM), leveraging Successive Interference Cancellation (SIC) and a Bit-Error-Rate (BER)-based automatic fallback—or "vertical handover"—mechanism. The proposed method monitors the instantaneous BER and dynamically switches between NOMA and OFDM based on predefined thresholds, maintaining optimal communication quality even under fading channel conditions. Unlike static multi-access systems, our approach adapts in real time to changing channel metrics, ensuring seamless transitions while minimizing performance degradation. Comparative analysis demonstrates that this hybrid handover design requires lower Signal-to-Noise Ratio (SNR) than existing schemes to maintain target BER performance, making it more practical and resilient in fading environments. The results highlight the potential for enhanced bandwidth and reliability in next-generation cellular systems by combining NOMA's power-domain multiplexing with OFDM's robustness to interference.

Keywords*: Bandwidth efficiency, Adaptive handover, NOMA, OFDM, Successive Interference Cancellation, Bit Error Rate (BER), Vertical Handover, Fading Channels.*

[1] *SAE (Society of Automotive Engineers), IEEE, Connected Vehicle, Fleet Telematics, Canton, MI, USA*

1. Introduction

With the advent of digital transmission, researchers have continuously sought efficient multiplexing schemes to meet the explosive growth in wireless data usage. Traditional approaches such as Frequency Division Multiplexing (FDM) allocate distinct frequency bands to multiple signals, requiring guard bands to prevent interference [1-2]. A more sophisticated approach, Orthogonal Frequency Division Multiplexing (OFDM), leverages orthogonal subcarriers to closely pack signals in the frequency spectrum, greatly enhancing bandwidth efficiency while avoiding guard bands[3-4].

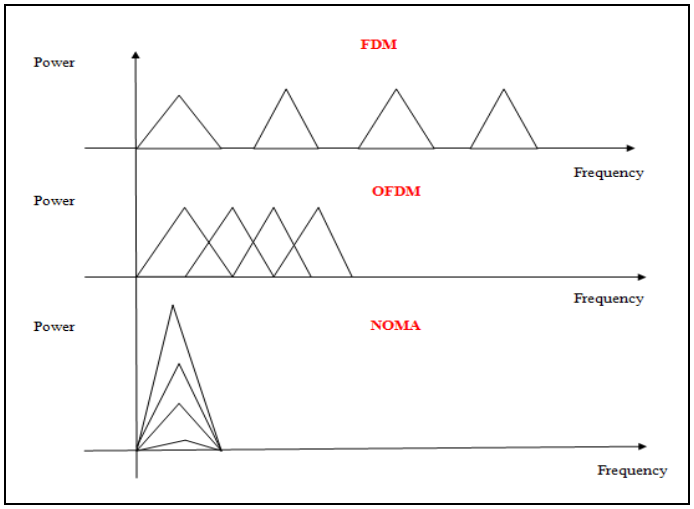

Fig.1 Spectrum of FDM, OFDM and NOMA

However, OFDM faces significant challenges chiefly a high Peak-to-Average Power Ratio (PAPR) [5], which strains power amplifiers, and stringent complexity requirements to maintain subcarrier orthogonality. Another classic approach, Time Division Multiplexing (TDM), was prominent in earlier wireless generations [6-8]. TDM sequences user data into time slots but suffers inefficiency in dynamic multi-user environments. As multimedia demand escalated, Non-Orthogonal Multiple Access (NOMA) emerged as a compelling innovation. By overlaying signals in the power domain rather than orthogonal domains, NOMA dramatically boosts spectral efficiency and supports massive connectivity [9]. Yet like OFDM, NOMA is also burdened by high PAPR and non-linear distortion effects due to hardware limitations. Modern cellular architectures often implement automatic fallback (vertical handover) to dynamically switch between coexisting technologies, ensuring reliable connectivity under varying Bit Error Rate (BER) conditions. This adaptability becomes feasible when systems such as NOMA and OFDM can operate over compatible bandwidths and exhibit comparable BER performance across selected SNR inversions [2, 4, 10-12].

In case of NOMA, signals are separated in the power domain. This necessitates the user signals to bear stark difference in power levels so that even while transmitting at the same frequency band and at same time slots, the separation among different signals can be accomplished [4]. The concept of Non-Orthogonal Multiple Access (NOMA) is depicted in figure 1.It can be observed from figure 1 that there is a large amount of bandwidth saving in case of using NOMA as compared with FDM and OFDM. A composite signal is however received at the receiving end of the cellular network which needs to separate out the signals. Considering x(t) be the transmitted signal, If N co-efficients are represented by A_1, A_2, A_3, A4...A_N and the strength of the reflections is a_1, a_2, a_3,.. , a_N then the weighted received signal y(t) is given by:

$$y(t) = a_1x(t) + a_2x(t - A_1) + \ \dots\dots aNx(t - A_{N)} + n(t) \qquad (1)$$

Here, n(t) represents additive interferences or noise effects.

Generally, the transmission channel is typically modeled digitally assuming a fixed sampling period T_s, thus equation (1) can be approximated as:

$$y(kT_s) = a_1u(kT_s) \ + a_2u(k_1T_s) + \cdots \ a_Nu(k - n)T_s + n(kT_s) \qquad (2)$$

Equation (2) assumes that the signal is sampled for every T_s time slot. The composite signal at the receiver needs to be separated in such a way that all users are detected with identical accuracy [5]. The metric which is generally considered to evaluate the performance of the system is the error rate. One of the major challenges which the NOMA based transmission faces is the reduction is power separation among signals due to fading and noise effects[6].

2. The Successive Signal Detection Approach

Typically, a wireless channel depicts frequency selective nature i.e. they behave differently for different frequencies. Moreover, the frequency selectivity is not fixed by also exhibits temporal variation [8]. This is depicted in figure 2.

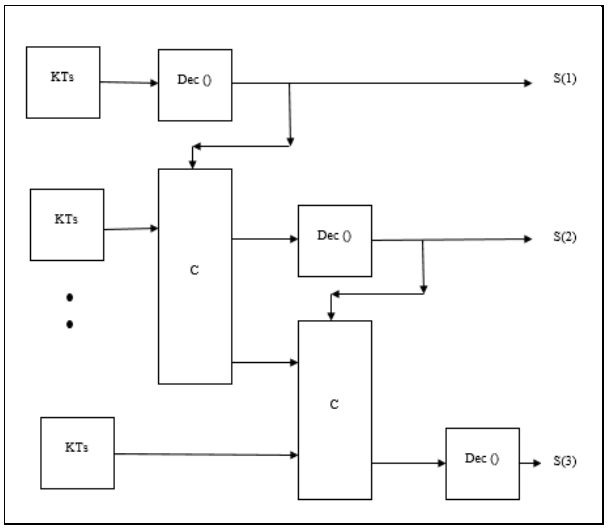

Fig. 2. The conceptual model for successive signal detection.

Where in Figure 2, KTs: It is the sampling block which samples the signal every KTs seconds, C: It is the canceller block, Dec(c): It is the decoder block. The successive signal detection mechanism is an iterative algorithm for the separation of signals in the power domain [13-14]. In this process, a multi-level comparison is made and the strongest signal is detected, stored and cancelled out from the composite signal. The detection starts with the strongest component and continues up to the weakest component. Since different paths have different gains given by (g), the received composite NOMA signal can be given by:

$$y(t) = x_1(t)g_1 + x_2(t)g_2 + \cdots .. x_n(t)g_n \quad (3)$$

Here in equation (3), $y(t)$ is the received composite NOMA signal, $x_n(t)g_n$ is the product of 'nth' transmitted signal with 'nth' path gain. Typically the following cases would arise: Near Users: The signals with the maximum path gains. Average Users: The signals with intermediate or average path gains. Far Users: The signals who have the least path gain. The different path gains actually arise out of the difference in the path lengths of the different users located at different locations in the cellular network [9]-[10]. The successive cancellation approach helps to detect the multiple signals separated in the power domain [11].

3. The Proposed System

The signals travelling through a wireless channel undergo the following detrimental effects: Multipath Propagation and Noise effetcs. Multipath propagation makes the channel impulse response a weighted sum of impulses and also results in the interference effects at the receiving end [12]-[13]. The following composite impulse response can be considered for such a wireless channel:

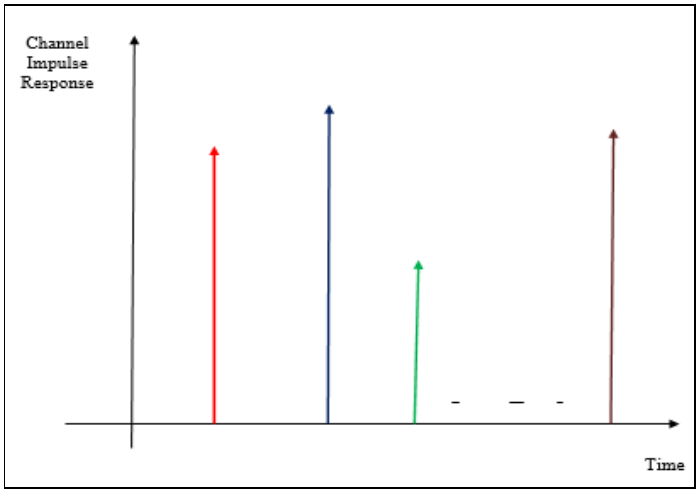

Fig. 3. Weighted impulse response of the channel

Mathematically, the composite impulse response of the channel can be given by:

$$h(t) = \sum_{i=1}^{n} \delta(t - i\tau g_i) \quad (4)$$

Here in Equation (4), $h(t)$ is the composite channel response, δ represents the impulse function, g_i is the weight or gain of the 'ith' path

τ is the delay in arrival of successive wave clusters due to multi-path propagation, and n is the total number of impulses.

The noise effects are considered to be Gaussian with a constant two-sided power spectral density (psd) given by:

$$psd_{noise} = \frac{N_0}{2} \nabla f : bandwidth \quad (5)$$

Here, in Equation (5), psd stands for the power spectral density, f stands for the frequency metric, N_0 is the one sided noise psd. The equalizer tries to nullify the effects of multi path propagation and noise effects. The equalization relies on the channel state information yielding the channel response (H). After obtaining the channel response (H), the inverse block is designed which is given in equation (6).

$$E = \frac{1}{H} \quad (6)$$

Here, in equation (6), E is the equalizer response, H is the sensed channel response, and the decision feedback equalizer (DFE) is employed in this approach which is depicted in figure 4.

The decision feedback equalizer adjusts the tap weights of the filter based on the actuating or error signal that is generated on comparing the dummy data transmitted and its copy received at the receiving end. The filter weights are updated every T_s seconds. In general, the sampling time of the receiver employing successive signal detection and that of the decision feedback equalizer are kept identical. Finally, the detection of the signals at the receiving end is done based on the following conditions:

$$Y_n(T_s) = \sum_{i=1}^{n} X_n(T_s) \quad (7)$$

Here, in equation (7), Y_n is the composite received signal, X_n represents the individual signals and T_s is the sampling time. The signals are detected from strongest to weakest as:

$$y_k = \max(Y_n(T_s) \quad (8)$$

Thus y_k is the strongest signal detected. It is stored and cancelled from the composite signal.

$$y^1 = Y_n(T_s) - y_k \quad (9)$$

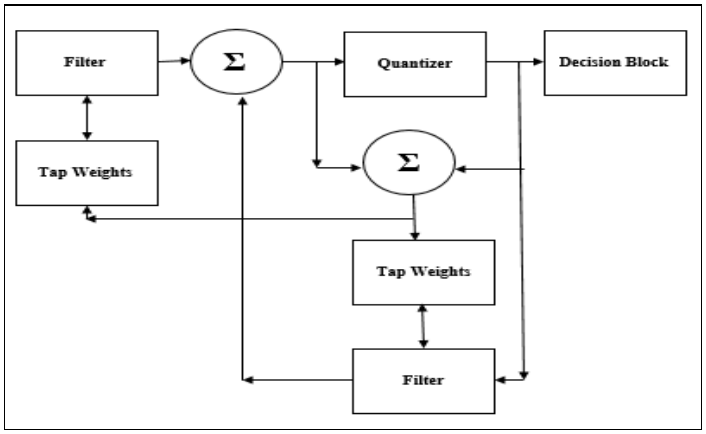

Fig. 4. Decision Feedback Equalizer [14]

Here, in equation (9), y^1 denotes the cancellation of the strongest after the first iteration. This process is continued iteratively till all the signals are detected. Typically, even with the use of equalizers and inter-leavers, noise effects cannot be mitigated completely. They act as reduction mechanisms. Signal fading effects result in outages and poor quality of service. Hence alternatives to restore quality of service are sought. One of the most effective techniques is the use of handover [15, 16-18]. Vertical handovers refer to the automatic fall-over from one technology to another in order to maintain communication. In cellular communication, candidates with similar QoS performance can be considered for handover. As far as 5G and onward technologies are concerned, OFDM and NOMA are suitable candidates due to their high spectral efficiency [19-22]. In case NOMA is the preferred candidate, an automatic fall back candidate can be considered to be OFDM. However, the choice of candidates to implement handover should satisfy the conditions of co-existence [16]. Showing that an identical SNR-BER curve can be achieved using OFDM and NOMA, thereby can justify co-existence of NOMA-OFDM for a cellular network which can lead to a possible vertical handover in case of system requirements. Non-identical BER performance in the SNR range would mean different characteristics for NOMA and OFDM thereby hindering handover. Based on the Automatic Fallback approach, choose the system BER as the metric to decide upon handover [23-26]. The system should ideally be designed for a near and far user case depicted in figure 5.

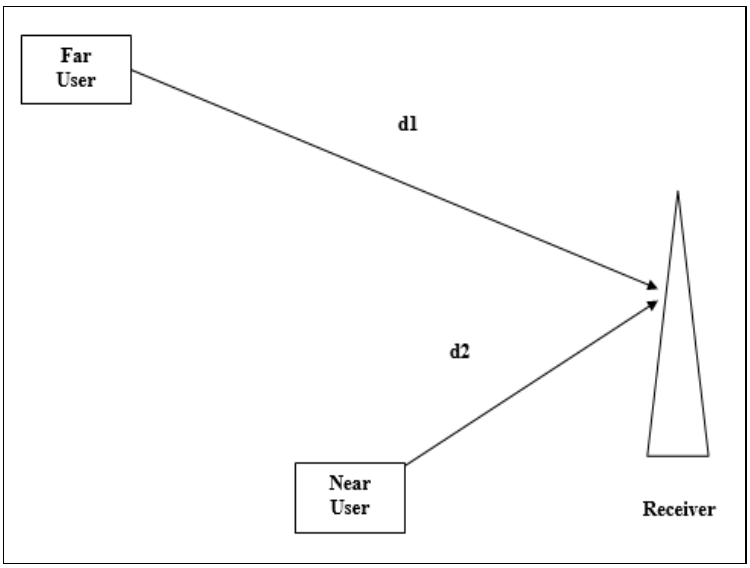

Fig. 5. The near and far user scenario in a wireless network

The near and far user scenario is differentiated by the path loss factor σ, where higher value of the path loss factor results in higher signal degradation and higher BER.The received signal at the receiver can represented as [17]:

$$r = X_0 h_0 \gamma_0 \sqrt{P_{TX,0}} + \sum_{i=1}^{n} X_i h_i \gamma_i \sqrt{P_{TX}} \quad (10)$$

Here, in equation (10), X is the interfering signal, h is the channel gain, γ is the lognormal shadowing effect, P_{TX} is the transmitted power, 'n' is the number of interferers. Typically, h is Raleigh distributed, in the dB domain, its Gamma distributed .γ is lognormal distributed, The subscript '0' represents the actual signal, The subscripts 'i' represent the set of interferers.

$X_0 h_0 \gamma_0 \sqrt{P_{TX,0}}$ and $X_i h_i \gamma_i \sqrt{P_{TX}}$ typically add up to a lognormal distributed

Random Variable. Hence the SNR can be easily computed. The correctness of signal reception depends on the following relation:

$$P(Power_{RX} \geq \gamma) \quad (11)$$

Here, in equation (11), P represents the probability, $Power_{RX}$ represents the received power, γ is the receiver threshold for reception (analogous to sensitivity). Typically, the OFDM/NOMA receiver would experience higher values of $Power_{RX}$ for near users compared to far users, but it would notbe constant due to channel and interference conditions. Hence, the decision to use a particular multiple access technique can notbe based on distance alone [18]. The proposed automatic fallback receiver is depicted in figure 6.

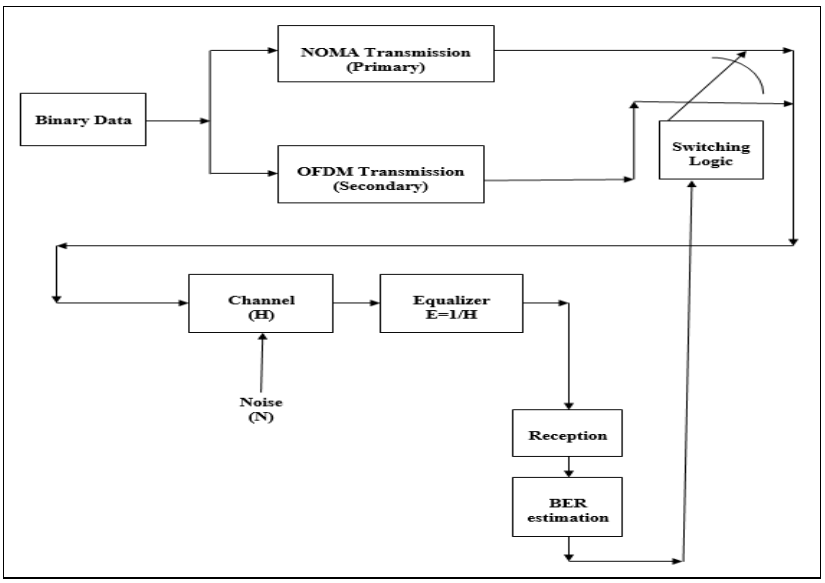

Fig. 6. The proposed system to implement automatic fallback between NOMA and OFDM

The automatic fallback mechanism estimates the BER of the system for both the competing techniques which are OFDM and NOMA and switches at the threshold of intersection of the NOMA-BER curves. The technique chosen is the one with the lesser BER.

4. Simulation Results and analysis

The simulations are carried out on Matlab 2020a. The multipath scenario is created with different paths corresponding to different path gains. It is assumed that the far users from the base station have the least path gain due to signal attenuation while the near users have the maximum path gain. The simulations are carried out for three cases. Such as: Strongest User without proposed system, Average User without proposed system, Average User witht proposed system, Weak User without proposed system and Weak user with proposed system.

It can be observed that without the proposed system, the BER of the strongest user falls steely while that

for the average and far users fall slowly. This implies that the near users or the users with maximum path gain can be detected with maximum accuracy and the signal of the rest of the users would bear more errors. However, with the proposed approach, the BER curves of all the users coincide thereby rendering the condition of ideal error rate and reliability of detection for all user cases.

Table 1: Performance Analysis of Proposed System and Conventional NOMA

S.No.	BER	SNR Range	Case
1	10^{-1}	0dB	Strongest User
2	10^{-1}	0dB	Weakest User without Proposed System
3	10^{-1}	0dB	Weakest User with Proposed System
4	10^{-1}	0dB	Average User without Proposed System
5	10^{-1}	0dB	Average User with Proposed System
6	10^{-2}	4dB	Strongest User
7	10^{-2}	10dB	Weakest User without Proposed System
8	10^{-2}	4dB	Weakest User with Proposed System
9	10^{-2}	8dB	Average User without Proposed System
10	10^{-2}	4dB	Average User with Proposed System
11	10^{-3}	7dB	Strongest User
12	10^{-3}	N.A.	Weakest User without Proposed System
13	10^{-3}	7dB	Weakest User with Proposed System
14	10^{-3}	11dB	Average User without Proposed System
15	10^{-3}	7dB	Average User with Proposed System
16	10^{-4}	8.2dB	Strongest User
17	10^{-4}	N.A.	Weakest User without Proposed System
18	10^{-4}	8.4dB	Weakest User with Proposed System
19	10^{-4}	N.A.	Average User without Proposed System
20	10^{-4}	8.2dB	Average User with Proposed System
21	10^{-5}	8.7dB	Strongest User
22	10^{-5}	N.A.	Weakest User without Proposed System
23	10^{-5}	10dB	Weakest User with Proposed System
24	10^{-5}	N.A.	Average User without Proposed System
25	10^{-5}	10dB	Average User with Proposed System

The BER curves for the different conditions tabulated in Table 1 are shown subsequently.

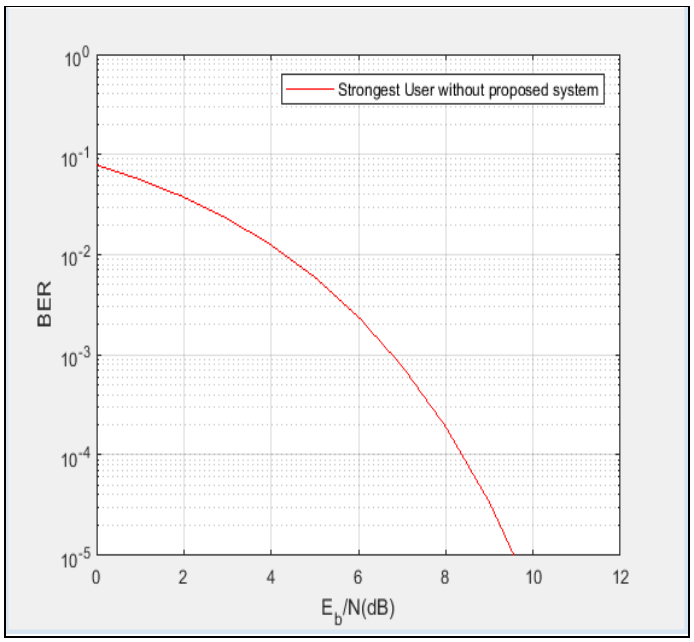

Fig. 7. Strongest user without proposed system

Figure 7 depicts the BER performance of the strongest or the nearest user from the base station. This line of propagation encounters the least attenuation among all multi path components.

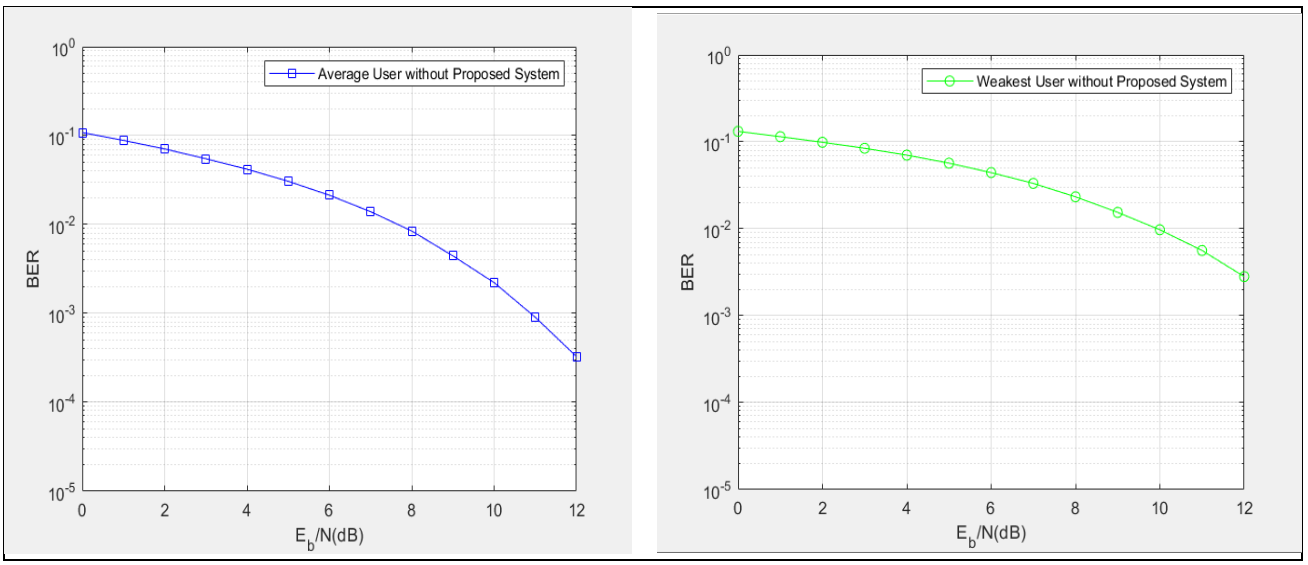

Fig. 8. BER Analysis for Average User without proposed system. Fig. 9. BER Analysis of Weakest User without proposed system.

Figure 8 depicts the BER performance of the average user from the base station. This multipath component encounters moderate attenuation. Figure 9 depicts the BER performance of the weakest user from the base station. This multipath component encounters the maximum attenuation. While figures 7, 8 and 9 depict the BER scenario for the multipath component mechanism scenario for conventional NOMA i.e. without the proposed system. figures 10 and 11 depict the BER scenario while employing the proposed NOMA detection mechanism. Figure 10 depicts the BER performance of the proposed system for the weakest user scenario. In contrast to the weakest user scenario without the proposed system, here the BER of the system falls steeply and becomes almost identical to the strongest user. Figure 11 depicts the BER performance of the proposed system for the average user scenario. In contrast to the average user scenario without the proposed system, here the BER of the system again falls steeply and becomes almost identical to the strongest user resembling the BER situation for the weakest user.

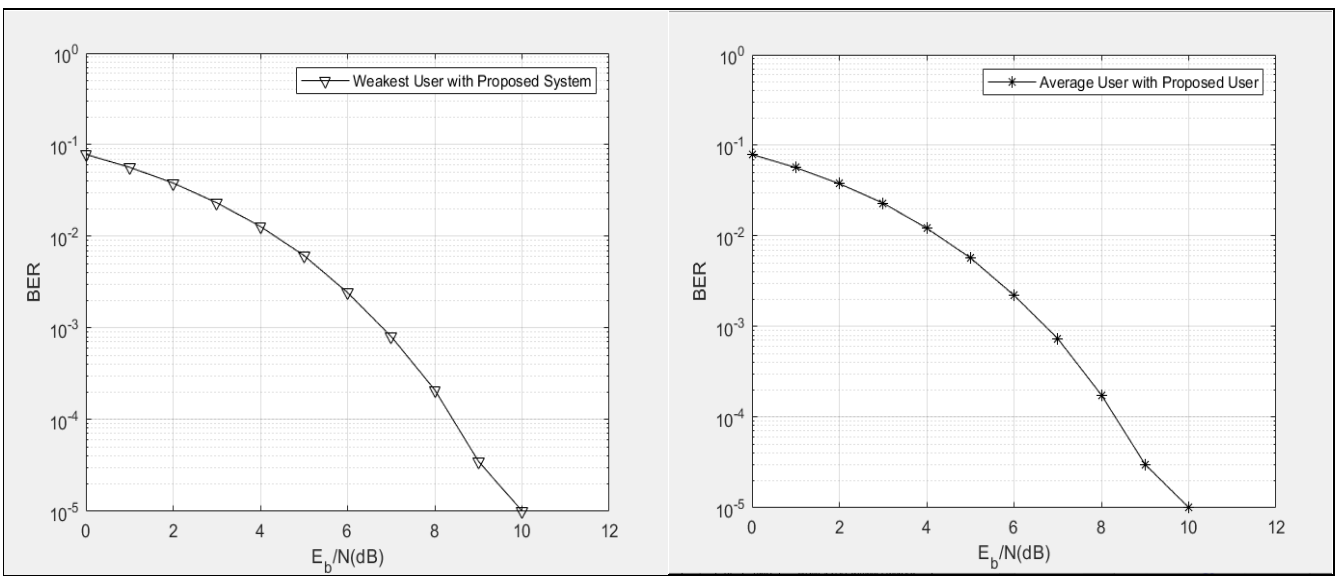

Fig. 10. BER Analysis of Weakest User with proposed system. Fig. 11. BER Analysis of Average User with proposed system.

A comparative BER analysis for the different conditions is depicted in figure 10. The simulation of BER has been operated for 10-1 to 10-5. The analysis could be obtained only for upto 10-5 as surpassing that value yielded relatively lower standards of communication quality in accordance with the Shannon's limit. It limit usually takes into account the errors for a BER range of 10-5 to 10-6 as negligible. The range of SNR has been selected as (0-12) dB attributing to the fact that there is convergence of the BER at around 10 dB. The term N.A here refers to not applicable and is generally refers to the case where it can't reach the particular BER value in the specified range of SNR. A comparative analysis based on graphical and tabular representation also represents an evaluation of the proposed system that legibly illustrates that after the implementation of the system proposed, the BER obtained for average and weak receivers is almost similar with respect the strong users at SNR ranges which are identical. That infers achieving better and improved Quality of Service for the NOMA systems that have been deployed. The automatic fall-back assisted handover characteristics are presented subsequently:

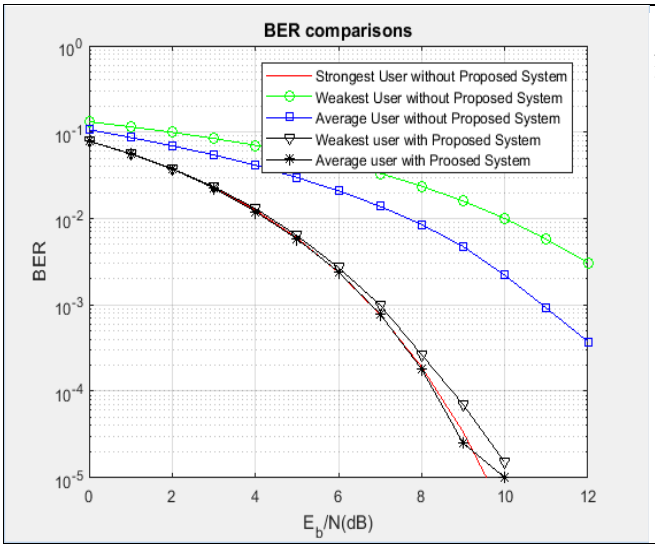

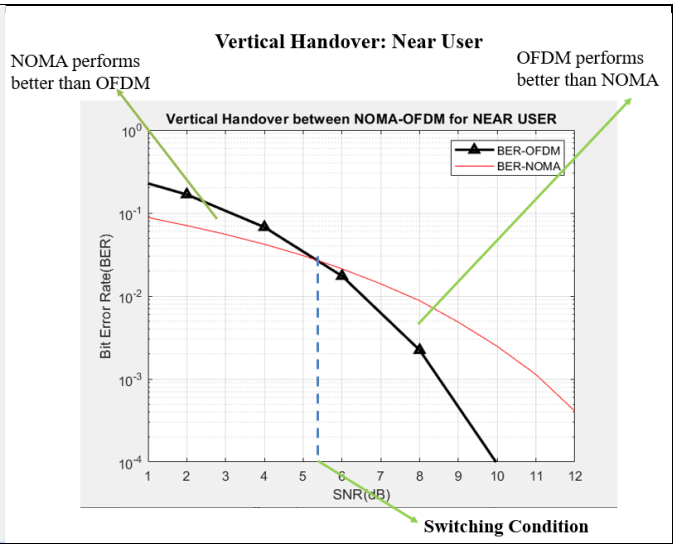

Fig. 12. Comparative BER Analysis of Proposed System for all user cases. Fig. 13. Near User Automatic Fallback,

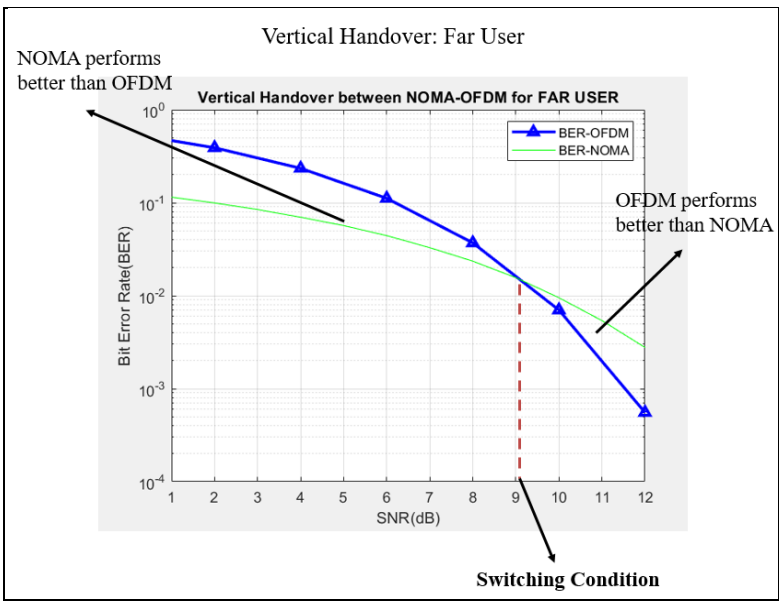

Fig. 14. Far User Automatic Fallback

Figure 13 depicts the situation wherein the optimal point of automatic fallback would be 5.4deciBel (from OFDM to NOMA) in case of the near user case. Figure 14 depicts the situation wherein the optimal point of automatic fallback would be 9deciBel (from OFDM to NOMA) in case of the far user case.

Clearly in the case of far users, the BER curve shows a sluggish plummeting nature compared to the near user case by dint of the fading effects in the channel. A comparative Analysis with contemporary techniques is presented in table 2. A comparative analysis with existing work clearly shows that indicates that the proposed system clearly outperforms the existing work in terms of SNR requirement, thereby making the system more practically suited for fading channels.

Table 2: Comparison with existing contemporary work

S.No	Authors	Findings
1.	A. Tusha et al. [15]	BER of 10^{-3} at SNR requirement of (12-15) dB (OFDM-NOMA-Near User) BER of 10^{-3} at SNR requirement of 20dB (OFDM-NOMA-Far User)
2.	Hussain et al. [16]	BER of 10^{-2} at SNR requirement of 20dB for PD-NOMA
3.	**Proposed Work**	BER of 10^{-3} at SNR requirement of 8.5dB (Proposed Technique-Near User) BER of 10^{-3} at SNR requirement of 11.5dB (Proposed Technique-Far User) BER of 10^{-2} at SNR requirement of 10dB for proposed NOMA scheme

5. Conclusion

This paper presents an automatic fallback mechanism for handover in wireless networks to implement vertical handover. The proposed technique is designed to minimize outages for fast fading channels. A practical multi user scenario is simulatedfor the proposed system with multi path propagation resulting in weighted impulse response model for the channel. The additional challenge addressed in this paper is the degradation of the BER of the system as the channel gain reduces with the distance of the user form the base station. A decision feedback equalization mechanism is employed to alleviate the non-ideal characteristics of the channel. It has been shown that in case of non-intersecting BER curves, the condition remains to be that of non-handover since one of the techniques for transmission continuously outperforms the other in terms of the performance metric (BER). In case of handover, concurrent BER curves for OFDM and NOMA intersect to create a point of intersection. The region prior to and subsequent to the intersection point govern the technology to be used. It has also been shown that the proposed technique outperforms existing approaches in the domain.

References

1. Y. Cai, Z. Qin, F. Cui, G. Y. Li, and J. A. McCann, “Modulation and multiple access for 5G networks,” *IEEE Communications Surveys & Tutorials*, vol. 20, no. 1, pp. 629–646, Q1 2018, doi: 10.1109/COMST.2017.2766698.
2. W. Shin, M. Vaezi, B. Lee, D. J. Love, J. Lee, and H. V. Poor, “Non-orthogonal multiple access in multi-cell networks: Theory, performance, and practical challenges,” *IEEE Communications Magazine*, vol. 55, no. 10, pp. 176–183, Oct. 2017, doi: 10.1109/MCOM.2017.1601065.
3. Z. Ding, X. Lei, G. K. Karagiannidis, R. Schober, J. Yuan, and V. K. Bhargava, “A survey on non-orthogonal multiple access for 5G networks: Research challenges and future trends,” *IEEE Journal on Selected Areas in Communications*, vol. 35, no. 10, pp. 2181–2195, Oct. 2017, doi: 10.1109/JSAC.2017.2725519.
4. Y. Chen, A. Bayesteh, Y. Wu, S. Han, M. Taherzadeh, D. Chen, and J. Ma, “SCMA: A promising non-orthogonal multiple access technology for 5G networks,” in *Proc. IEEE 84th Vehicular Technology Conference (VTC-Fall)*, Sept. 2016, pp. 1–6, doi: 10.1109/VTCFall.2016.7881213.
5. J. Choi, J. Mo, and R. W. Heath, “Near maximum-likelihood detector and channel estimator for uplink multiuser massive MIMO systems with one-bit ADCs,” *IEEE Transactions on Communications*, vol. 64, no. 5, pp. 2005–2018, May 2016, doi: 10.1109/TCOMM.2016.2545666.
6. Y. Tao, L. Liu, S. Liu, and Z. Zhang, “A survey: Several technologies of non-orthogonal transmission for 5G,” *China Communications*, vol. 12, no. 10, pp. 1–15, Oct. 2015, doi: 10.1109/CC.2015.7315054.

7. A. Benjebbour, K. Saito, A. Li, K. Kishiyama, and T. Nakamura, "Non-orthogonal multiple access (NOMA): Concept, performance evaluation and experimental trials," in *Proc. International Conference on Wireless Networks and Mobile Communications (WINCOM)*, Aug. 2015, pp. 1–6, doi: 10.1109/WINCOM.2015.7381343.
8. L. Wei, Q. Hu, Y. Qian, and G. Wu, "Key elements to enable millimeter wave communications for 5G wireless systems," *IEEE Wireless Communications*, vol. 21, no. 6, pp. 136–143, Dec. 2014, doi: 10.1109/MWC.2014.7000981.
9. P. S. Lu, X. Zhou, and T. Matsumoto, "Outage probabilities of orthogonal multiple-access relaying techniques with imperfect source-relay links," *IEEE Transactions on Wireless Communications*, vol. 14, no. 4, pp. 2269–2280, Apr. 2015, doi: 10.1109/TWC.2014.2384046.
10. Y. Saito, Y. Kishiyama, A. Benjebbour, T. Nakamura, A. Li, and K. Higuchi, "Non-orthogonal multiple access (NOMA) for cellular future radio access," in *Proc. IEEE 77th Vehicular Technology Conference (VTC Spring)*, Dresden, Germany, June 2013, pp. 1–5, doi: 10.1109/VTCSpring.2013.6692652.
11. A. Benjebbour, Y. Saito, Y. Kishiyama, A. Li, A. Harada, and T. Nakamura, "Concept and practical considerations of non-orthogonal multiple access (NOMA) for future radio access," in *Proc. International Symposium on Intelligent Signal Processing and Communication Systems (ISPACS)*, Dec. 2013, pp. 770–774, doi: 10.1109/ISPACS.2013.6704653.
12. J. Umehara and Y. Kishiyama, "Enhancing user fairness in non-orthogonal access with successive interference cancellation for cellular downlink," in *Proc. IEEE International Conference on Communication Systems (ICCS)*, Singapore, Nov. 2012, pp. 324–328, doi: 10.1109/ICCS.2012.6406163.
13. M. F. Mesiya, *Contemporary Communication Systems*, 2nd ed. New York, NY, USA: McGraw-Hill.
14. B. P. Lathi, *Modern Digital and Analog Communication Systems*, 4th ed. New York, NY, USA: Oxford University Press.
15. A. Tusha, S. Doğan, and H. Arslan, "A hybrid downlink NOMA with OFDM and OFDM-IM for beyond 5G wireless networks," *IEEE Signal Processing Letters*, vol. 27, pp. 491–495, Mar. 2020, doi: 10.1109/LSP.2020.2979059.
16. M. Hussain and H. Rasheed, "Nonorthogonal multiple access for next-generation mobile networks: A technical aspect for research direction," *Wireless Communications and Mobile Computing*, vol. 2020, Art. no. 8845371, pp. 1–17, 2020.
17. Y. Yapıcı and I. Güvenç, "NOMA for VLC downlink transmission with random receiver orientation," *IEEE Transactions on Communications*, vol. 67, no. 8, pp. 5558–5573, Aug. 2019.
18. K. Vasudeva, K. Simsek, D. López-Pérez, and I. Güvenç, "Analysis of handover failures in heterogeneous networks with fading," *IEEE Transactions on Vehicular Technology*, vol. 66, no. 7, pp. 6060–6074, July 2017.
19. S. Patel, "Performance analysis of acoustic echo cancellation using adaptive filter algorithms with Rician fading channel," *International Journal of Trend in Scientific Research and Development*, vol. 6, no. 2, pp. 1541–1547, Feb. 2022, doi: 10.5281/zenodo.11195267.
20. P. Gupta, M. Patidar, and P. Nema, "Performance analysis of speech enhancement using LMS, NLMS and UNANR algorithms," in *Proc. International Conference on Computing, Communication and Control (IC4)*, Indore, India, 2015, pp. 1–5, doi: 10.1109/IC4.2015.7375561.
21. S. Patel, "Enhancing image quality in wireless transmission through compression and de-noising filters," *International Journal of Trend in Scientific Research and Development*, vol. 5, no. 2, pp. 415–422, Apr. 2021.

22. M. Patidar *et al*., "An ultra-area-efficient ALU design in QCA technology using synchronized clock zone scheme," *Journal of Supercomputing*, pp. 1–30, 2022, doi: 10.1007/s11227-022-04567-8.

23. M. Patidar *et al*., "An empirical study and simulation analysis of the MAC layer model using the AWGN channel on WiMAX technology," in *Proc. 2nd International Conference on Technology Advances in Computer Science (ICTACS)*, Tashkent, Uzbekistan, 2022, pp. 658–662, doi: 10.1109/ICTACS56270.2022.9988033.

24. M. Patidar *et al*., "Performance analysis of WiMAX 802.16e physical layer model," in *Proc. 9th International Conference on Wireless and Optical Communications Networks (WOCN)*, Indore, India, 2012, pp. 1–4, doi: 10.1109/WOCN.2012.6335540.

25. S. Patel, "Optimizing wiring harness minimization through integration of Internet of Vehicles (IoV) and Internet of Things (IoT) with ESP-32 module: A schematic circuit approach," *International Journal of Research Trends and Innovation (IJRTI)*, vol. 8, no. 9, pp. 95–103, Sep. 2023.